

## **Fundamental Mode Approach to Forward Problem Solutions in EMI Scattering ---- Inferring fundamental solutions from training data**

K. Sun<sup>(1)</sup>, K O'Neill<sup>(1,2)</sup>, F. Shubitidze<sup>(1)</sup>, I. Shamatava<sup>(1)</sup>, K. D. Paulsen<sup>(1)</sup>

(1) Thayer School of Engineering, Dartmouth College, Hanover NH, 03755, USA

(2) USA ERDC Cold Regions Research and Engineering Laboratory  
72 Lyme Road, Hanover NH, 03755, USA

Keli.sun@dartmouth.edu

**Abstract** Electromagnetic induction (EMI: 10's of Hz to 100's of kHz) is the leading technology for discrimination of subsurface metallic targets such as unexploded ordnance (UXO). The cleanup problem requires solution of remote sensing inverse problem inevitably based on some very fast forward algorithms for calculating EMI. The forward model must determine responses of arbitrarily complicated metallic objects. Here a very fast and complete forward solution system is presented, based on fundamental mode excitations. For a given target (or a set of targets), the EMI responses to fundamental modes are obtained from training data and saved. Any realistic excitation field is then decomposed into a limited number of constituent fundamental modes and the scatterer's EMI response is obtained by superposition of the fundamental mode solutions. In this paper we define the fundamental excitations explicitly and consider their rationale; show how to construct any particular solutions from solutions to the fundamental excitations; and focus particularly on how to obtain, retain, express responses to the fundamental solutions in the face of inherent ill-conditioning.

## **1 Introduction**

Cleanup of UXO sites is extremely expensive because of high false alarm rates. Given that there are over 10,000,000 acres of land with potential UXO hazard in the US alone, reliable techniques for UXO discrimination are urgently needed. As an inverse problem, UXO discrimination requires a fast forward model, i.e. a model calculating EMI responses for prospective targets that may be present. Many numerical techniques are available for EMI calculation in the magneto-quasistatic EMI regime, but most of them are not fast enough for inversion or complete enough to deal with realistic objects. One of the most successful models is the dipole model [1,2], in which one approximates a target's response with one or a number of infinitesimal magnetic dipoles, each responding independently to the local value of the transmitted ("primary") field that strikes it. The dipole model is a good approximation only if the observation position is far enough from the target and if the parts of the object do not interact significantly. However, in UXO detection and discrimination the sensor is often close to the target, and we have shown elsewhere that interaction effects can be very significant [3, 4]. Fast analytical solution for a spheroid in EMI frequencies range has been developed recently [5,6] and a spheroid model was shown to be capable of representing effectively some geometrically complex objects [7,8]. The spheroid model has two advantages: (1) It takes the near field effect into account, so it can also be used when the sensor is close; and (2) the target information (geometrical dimension, orientation, conductivity, magnetic permeability, etc.) can be estimated directly from model parameters.

For more complicated, materially heterogeneous objects, the dipole or spheroid models are not wholly adequate, and detailed numerical solution by established method is too slow. The alternative is a

Report Documentation Page				Form Approved OMB No. 0704-0188	
Public reporting burden for the collection of information is estimated to average 1 hour per response, including the time for reviewing instructions, searching existing data sources, gathering and maintaining the data needed, and completing and reviewing the collection of information. Send comments regarding this burden estimate or any other aspect of this collection of information, including suggestions for reducing this burden, to Washington Headquarters Services, Directorate for Information Operations and Reports, 1215 Jefferson Davis Highway, Suite 1204, Arlington VA 22202-4302. Respondents should be aware that notwithstanding any other provision of law, no person shall be subject to a penalty for failing to comply with a collection of information if it does not display a currently valid OMB control number.					
1. REPORT DATE <b>23 APR 2004</b>		2. REPORT TYPE <b>N/A</b>		3. DATES COVERED <b>-</b>	
4. TITLE AND SUBTITLE <b>Fundamental Mode Approach to Forward Problem Solutions in EMI Scattering ---- Inferring fundamental solutions from training data</b>				5a. CONTRACT NUMBER	
				5b. GRANT NUMBER	
				5c. PROGRAM ELEMENT NUMBER	
6. AUTHOR(S)				5d. PROJECT NUMBER	
				5e. TASK NUMBER	
				5f. WORK UNIT NUMBER	
7. PERFORMING ORGANIZATION NAME(S) AND ADDRESS(ES) <b>Thayer School of Engineering, Dartmouth College, Hanover NH, 03755, USA</b>				8. PERFORMING ORGANIZATION REPORT NUMBER	
9. SPONSORING/MONITORING AGENCY NAME(S) AND ADDRESS(ES)				10. SPONSOR/MONITOR'S ACRONYM(S)	
				11. SPONSOR/MONITOR'S REPORT NUMBER(S)	
12. DISTRIBUTION/AVAILABILITY STATEMENT <b>Approved for public release, distribution unlimited</b>					
13. SUPPLEMENTARY NOTES <b>See also ADM001763, Annual Review of Progress in Applied Computational Electromagnetics (20th) Held in Syracuse, NY on 19-23 April 2004., The original document contains color images.</b>					
14. ABSTRACT					
15. SUBJECT TERMS					
16. SECURITY CLASSIFICATION OF:			17. LIMITATION OF ABSTRACT <b>UU</b>	18. NUMBER OF PAGES <b>8</b>	19a. NAME OF RESPONSIBLE PERSON
a. REPORT <b>unclassified</b>	b. ABSTRACT <b>unclassified</b>	c. THIS PAGE <b>unclassified</b>			

fundamental mode approach [3,9,10]. We choose a set of fundamental excitation modes whose linear combination can represent an arbitrary excitation field. The EMI response of the target to each fundamental mode is obtained and stored. Since the system we are studying is linear, if some general excitation field constitutes a particular superposition (linear combination) of inputs, the response will be a corresponding superposition of outputs. So one just needs to build a library for known UXOs, where the fundamental solutions (i.e. the response of each UXO to fundamental excitation modes) are stored. The EMI response of any UXO to an arbitrary excitation can then be easily constructed from the library data. There are two main approaches to obtain the fundamental solutions: (1) for relatively simple object whose components (geometry and electromagnetic properties of each parts) are known, the fundamental solution can be calculated directly through numerical simulation [3]. (2) For the more general case, the fundamental solution can be obtained indirectly from properly designed measurements (so called training data). A major difficulty in the fundamental mode approach is that the excitation fields from realistic EMI sensors are usually a combination of the fundamental modes, so the fundamental solution has to be solved through an inversion procedure, which often suffers from ill-conditioning. In this paper, we will first introduce a selected set of fundamental modes and two approaches for inferring fundamental solutions from the training data. Then we show two approaches to treat the ill-conditioning problem and demonstrate some results.

## 2 Fundamental mode approach

### 2.1 Expressing arbitrary primary fields using fundamental modes

As elaborated elsewhere [11,12], in the EMI band we can usually consider the magnetic fields in the air and soil to be irrotational, with the result that they can be expressed as gradients of a scalar potential that satisfies the Laplace equation. Because UXO are typically elongated bodies of revolution, we choose Associated Legendre functions in prolate spheroidal coordinates as the fundamental solution forms. On a spheroid surface away from the sensor, the primary EMI potential field can be written as a summation of fundamental modes:

$$\psi^{pr} = \frac{H_0 d}{2} \sum_m \sum_{n=m}^{\infty} \sum_{p=0}^1 b_{pmn} P_n^m(\eta) P_n^m(\xi_0) T_{pm}(\phi) = \sum_{k=1}^K b_k \psi_k^{pr}(\eta, \xi_0, \phi) \quad (1)$$

where here and in what follows the coordinate system is centered on the scatterer,  $(\eta, \xi, \phi)$  are the standard spheroidal coordinates,  $d$  is the inter-focal distance,  $P_n^m$  is Associated Legendre functions of the first, of order  $m$  and degree  $n$ .  $T_{pm}(\phi)$  is  $\cos(m\phi)$  for  $p = 0$  and is  $\sin(m\phi)$  for  $p = 1$ . The coefficients  $b_{pmn}$  can be obtained by using orthogonality relations for the Legendre functions. For the purpose of simplicity, we rewrite the series in the middle of (1) using a condensed subscript notation on the right, with  $k = n - m + 1 + m \cdot n_{\max} + p \cdot (m_{\max} + 1) \cdot n_{\max}$ . In practice, the series will be truncated, i.e. we will only consider terms:  $0 \leq p \leq 1$ ,  $0 \leq m \leq m_{\max}$ ,  $m \leq n \leq m + n_{\max} - 1$ . To proceed for an arbitrary object, we define a spheroidal surface  $S$  surrounding the object, more or less conforming to its general shape, i.e. we choose some suitable  $d$  and  $\xi_0$ , though the details of that choice are not critical.

### 2.2 Constructing general responses using fundamental solutions

As for primary field, the scattered field outside of the target (as well as the exterior of the auxiliary spheroid) is irrotational and the scattered field potential function satisfies Laplace equation. For each fundamental excitation  $\psi_k^{pr}$ , we represent the corresponding scattered field with a number of magnetic

charges located on (or inside) the auxiliary spheroid surface, i.e. the scattered potential fields corresponding to excitation  $\psi_k^{pr}$  at location  $\mathbf{R}$  are

$$\psi_k(\mathbf{R}) = \sum_{i=1}^{N_{source}} \frac{\rho_k^i}{4\pi\mu_0 |\mathbf{R} - \mathbf{R}_i|} \quad (2)$$

and the total scattered magnetic field will be

$$\mathbf{H}(\mathbf{R}) = \sum_k b_k \sum_i \frac{\rho_k^i}{4\pi\mu_0 |\mathbf{R} - \mathbf{R}_i|^3} (\mathbf{R} - \mathbf{R}_i) \quad (3)$$

The magnetic charges  $\rho_k^i$  are obtained by the methods described below and then stored before attacking any particular application. When arbitrary excitation fields are decomposed into basic modes (i.e. the  $b_k$  are determined), then the scattered field can be easily computed by superposition (i.e. by (3)). One of the essential steps is to obtain the fundamental solutions in the first place, which will be demonstrated in the next section.

## 2.3 Inferring fundamental solutions from training data

In numerical simulation, EMI response of a specific target to each fundamental excitation  $\psi_j^{pr}$  can be calculated individually. However, it is not the case in real measurement because our instruments do not transmit individual fundamental excitation modes, one by one. The field from realistic sensor is usually a combination of a number of fundamental modes. To approach this, we consider below the particular GEM-3 sensor developed by Geophex Ltd.[13], which has distinguished itself in UXO discrimination application.

### 2.3.1 Simple least squares approach

The GEM-3 we are currently using is mono-static and measures only the component of the scattered field normal to the sensor head, so the forward model is expressed as:

$$H_j = \sum_k b_k^j \sum_i \frac{\rho_k^i}{4\pi\mu_0 |\mathbf{R}_j - \mathbf{R}_i|^3} (\mathbf{R}_j - \mathbf{R}_i) \cdot \mathbf{N}_j \quad (4)$$

Where  $j$  is the index of the position  $\mathbf{R}_j$  where that normal field was measured, and  $\mathbf{N}_j$  is the direction normal to sensor head at point  $\mathbf{R}_j$ .

For given a set of training data (well designed measurements for a specific target),  $\rho_{pmn}^i$  can be determined by minimizing

$$MSQ = \sum_j |H_j - H_j^d|^2 = \sum_j \left| \sum_k b_k^j \sum_i \frac{\rho_k^i}{4\pi\mu_0 |\mathbf{R}_j - \mathbf{R}_i|^3} (\mathbf{R}_j - \mathbf{R}_i) \cdot \mathbf{N}_j - H_j^d \right|^2 \quad (5)$$

Using a least square error approach, we can build the normal equations

$$\mathbf{A} \mathbf{q} = \mathbf{b} \quad (6)$$

by setting  $\frac{\partial MSQ}{\partial \rho_k^i} = 0$ , i.e.

$$\begin{aligned} A_{l',l} &= \sum_j \left( \sum_k b_k^j \sum_i \frac{1}{4\pi\mu_0 |\mathbf{R}_j - \mathbf{R}_i|^3} (\mathbf{R}_j - \mathbf{R}_i) \cdot \mathbf{N}_j \right) b_{k'}^j \frac{(\mathbf{R}_j - \mathbf{R}_{i'}) \cdot \mathbf{N}_j}{|\mathbf{R}_j - \mathbf{R}_{i'}|^3} \delta_{i'k',l'} \delta_{ik,l} \\ b_{l'} &= \sum_j H_j^d b_{k'}^j \frac{(\mathbf{R}_j - \mathbf{R}_{i'}) \cdot \mathbf{N}_j}{|\mathbf{R}_j - \mathbf{R}_{i'}|^3} \delta_{i'k',l'} \quad q_l = \rho_k^i \delta_{ik,l} \end{aligned} \quad (7)$$

Here we define

$$\delta_{ik,l} = \begin{cases} 1 & \text{if } l = n - m + 1 + m \cdot n_{\max} + p(m_{\max} + 1)n_{\max} + 2(i-1)(m_{\max} + 1)n_{\max} \\ 0 & \text{other} \end{cases} \quad (8)$$

The magnetic charge magnitude  $\rho_k^i$  (or  $\mathbf{q}$ ) can be obtained by solving (6).

### 2.3.2 Levenberg-Marquardt (LM) approach

As we will show in the results section, the inverse problem is usually highly ill conditioned. For this reason, we employ LM approach [14], where the magnetic charge magnitudes  $\mathbf{q}$  are obtained through iteration with a regularization factor  $\lambda$ :

$$\mathbf{q}^{(k+1)} = \mathbf{q}^{(k)} + (\mathbf{J}^T \mathbf{J} + \lambda \mathbf{I})^{-1} [\mathbf{J}^T (\mathbf{H}^d - \mathbf{H})] \quad (9)$$

Where  $\mathbf{H}^d$  is the measurement data,  $\mathbf{H} = \mathbf{H}(\mathbf{q})$  is the modeled value, and the Jacobian matrix  $\mathbf{J} = \frac{\partial \mathbf{H}}{\partial \mathbf{q}}$ .

## 3 Results

### 3.1 Inherent ill-conditioning

In general, the excitation field from a realistic EMI sensor contains mainly a small number of basic modes, with the contribution of other modes (usually high order modes) negligibly small. As an example, Figure 1a shows the coefficients of basic modes  $b_{pmn}$  from GEM-3 for a spheroid with equation  $(x/0.03)^2 + (z/0.18)^2 = 1$ . The index is lined up according to the formulation  $k = n - m + 1 + m \cdot n_{\max} + p \cdot (m_{\max} + 1) \cdot n_{\max}$  with  $n_{\max} = 5$ ,  $m_{\max} = 3$ . The first term  $b_{000}$  does not induce any scattering. So in this case the dominant terms are  $b_{001}$  ( $k=2$ , corresponding to uniform axial excitation),  $b_{011}$  ( $k=6$ , uniform transverse excitation) and several other small terms. All the other terms are

essentially zero. Figure 1b is similar except that the sensor moves along a cubic box surrounding the spheroid and the summation of the coefficients  $b_{pmn}$  from all positions are plotted. For both cases we see that the coefficients of many terms are very small compared to the dominant ones.

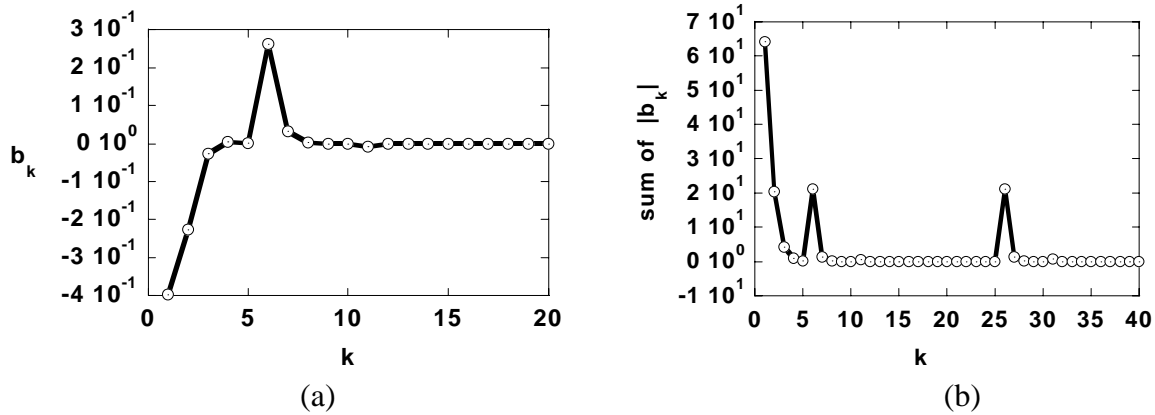
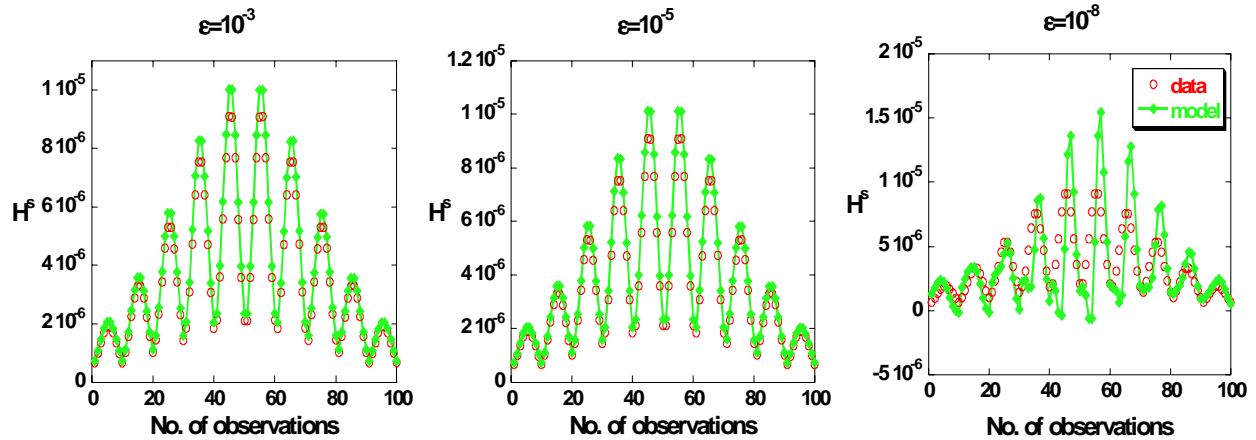


Figure 1 a) coefficient of fundamental modes  $b_{pmn}$ , when the spheroid is 30 cm from the 40 cm diameter GEM-3 sensor and is tilted from the horizontal at  $45^\circ$ . b) Summation of  $|b_{pmn}|$  over all observations, as the sensor moves over a 90 cm square cube surrounding the spheroid.

### 3.2 Least square approach

As shown in previous section, the training data contains very little information on high order excitation modes. The consequence is that EMI data in this set of training data is not sensitive to the fundamental solution of these terms, i.e.  $\partial \mathbf{H} / \partial q_k$  is close to zero, so that the matrix  $\mathbf{A}$  in (6) is singular and the equation cannot be solved accurately. Fortunately, these high order terms also typically contribute very little in actual applications, so that the accurate fundamental solution of these terms is not necessary. This allows us to simply truncate these non-essential terms to reduce singularity. In this least squares approach, we define the criterion of truncation as  $|b_k| / \max |b_k| \leq \varepsilon$ , where  $\max |b_k|$  is the maximum of all coefficients except  $k = 1$ . Figure 2 shows an example of the field reconstruction for different values of  $\varepsilon$ . The target is an ellipsoid given by  $(x/0.01)^2 + (y/0.03)^2 + (z/0.18)^2 = 1$  and the surrounding spheroid is  $(x/0.03)^2 + (z/0.18)^2 = 1$ . The training data were measured along a cubic box with surfaces at  $x = \pm 0.45m$ ,  $y = \pm 0.45m$ , and  $z = \pm 0.45m$ , with 100 measurements on each surface. Instead of actual measurements, the training data in this paper were synthetic ones calculated by the TSA code [11]. To better understand the spheroid position relative to measurement grid, we adopt the notation of Euler Angles  $(\theta, \phi, \psi)$  [15]. This box measurement is equivalent to fixing the rectangular grid corresponding to a side of the box and changing the center location  $(x_0, y_0, z_0)$  and orientation of the target and spheroid as follows:  $x_0 = 0$ ,  $y_0 = 0$ ,  $z_0 = -45cm$ ,  $(\theta_1, \phi_1, \psi_1) = (0, 0, 0)$ ,  $(\theta_2, \phi_2, \psi_2) = (\pi, 0, 0)$ ,  $(\theta_3, \phi_3, \psi_3) = (\pi/2, 0, 0)$ ,  $(\theta_4, \phi_4, \psi_4) = (\pi/2, 0, \pi/2)$ ,  $(\theta_5, \phi_5, \psi_5) = (\pi/2, 0, \pi)$ ,  $(\theta_6, \phi_6, \psi_6) = (\pi/2, 0, 3\pi/2)$ .



**Figure 2** EMI response constructed from fundamental solutions (green markers) compared to synthetic data (circles)

To produce the fundamental mode solutions, 11 point charges are distributed uniformly in space on the surrounding spheroid surface. The fundamental solutions were obtained from the training data via (6). To check the accuracy of the inferred fundamental solutions, we calculated the EMI response along rows of observation points over the grid, with the central rows passing over the target, producing the serrated response pattern in Figure 2, which shows results for the phase quadrature component of 47970 Hz excitation. The target parameters are  $(\theta, \phi, \psi) = (\pi/2, 0, 0)$ ,  $x_0 = y_0 = 0$ ,  $z_0 = -60\text{cm}$ . The truncation criteria factors are  $\varepsilon = 10^{-3}$ ,  $10^{-5}$ , and  $10^{-8}$ . Results show that we can obtain reasonably accurate fundamental solutions by choosing a proper truncation criterion (i.e.  $10^{-3}$  and  $10^{-5}$  in this case). Our neglecting the truncated terms causes the remaining small error in the best results. As the truncation criterion becomes too small, the high order terms begin to induce singularity and may destroy the whole solution.

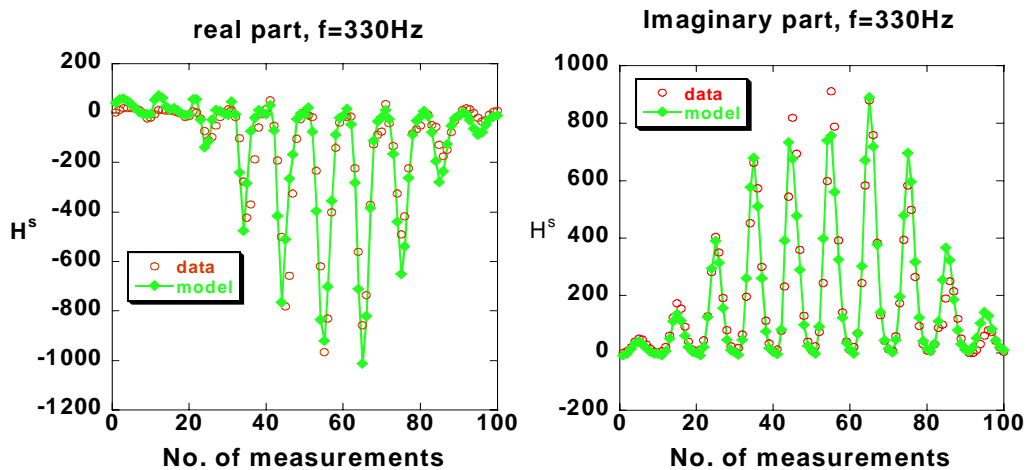


**Figure 3** EMI response constructed from fundamental solutions (green markers) compared to measurements (circles)

Figure 3 showed results of a standard 81cm UXO for both real and imaginary part at 330Hz. The UXO is centered on  $(-5, -5, -30)$  cm in the measurement grid coordinate, with a horizontal

orientation:  $(\theta, \phi, \psi) = (\pi/2, \pi/2, 0)$ . The training data are 3 set of measurements: (1) centered at  $(-5, 0.66, -39.48)$ cm, angle  $(\theta, \phi, \psi) = (7\pi/36, \pi/2, 0)$  (2)  $(-5, 0.66, -39.48)$ cm, angle  $(\theta, \phi, \psi) = (29\pi/36, 3\pi/2, 0)$  (3) center at  $(-5, -5, -20)$  cm, angle  $(\theta, \phi, \psi) = (\pi/2, \pi/2, 0)$ . The fundamental solutions are calculated with truncation parameter  $\varepsilon = 10^{-4}$  and the modeled data match with measured ones pretty well. It should be noticed that the testing data is close to one set of training data (set 3). For more complete test of the model accuracy, more general measurements need to be done for comparison.

### 3.3 LM approach

Instead of simply truncating the “non-essential” terms (which is equivalent to setting their solution to be zero), in the LM approach we keep these terms and the iterative procedure will assign them some reasonable values, which produces more accurate solutions than simple truncation. This regularization factor  $\lambda$  makes sure that their value won't become so erratic as to cause instability. For the same set of training data as in section 3.2, we set an initial value for  $\lambda$ , reducing it as the iteration proceeds. Once the error term stops decreasing, we set the regularization factor back to initial value and iterate again [16]. Experience shows that the solution is not very sensitive to  $\lambda r$  and results are more accurate and stable than those from the least squares approach. Some examples are shown in as shown in Figure 4 .

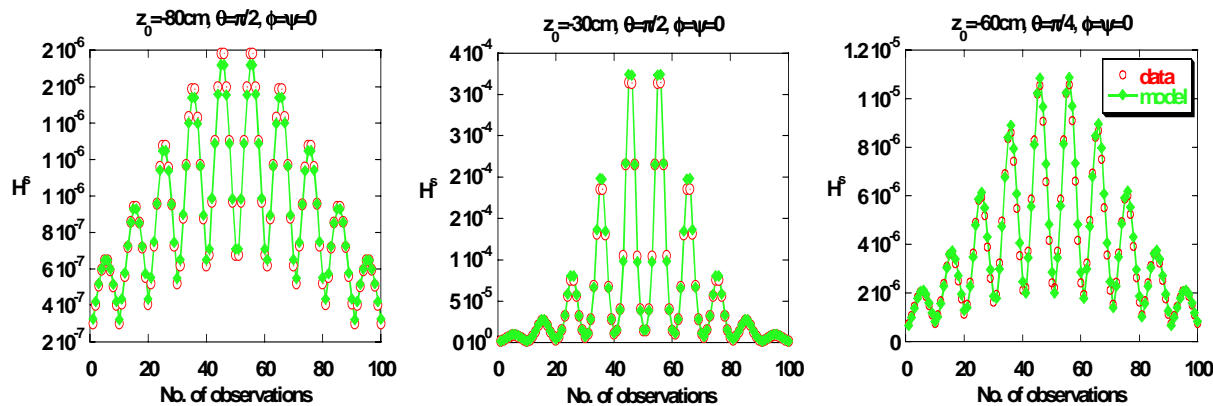


Figure 4. EMI response constructed from fundamental solutions (green markers) compared to synthetic data (circles), based on the LM approach.

## 4 Concluding discussion

A fundamental mode approach was developed for fast calculation of the complete EMI response of complicated 3D objects. For prospective targets, the fundamental solutions are obtained and stored in library. The response of these targets to arbitrary EMI excitation can then be constructed quickly by simple superposition of the fundamental solutions. Two approaches to infer fundamental solutions from training data (usually measurement data) were introduced: simple least squares error minimization and a Levenberg-Marquardt approach. Both approach give reasonable results if inversion control parameters are properly used. While the preliminary results are promising, further study is needed to make the approach more efficient and practical. More realistic targets need to be studied to determine the criteria for truncation and regularization parameters. We also seek better ways of distributing the magnetic charges to



reduce the number of unknowns and the computational cost. A better design of training data (especially bi-static data or data for three components of  $H$ ) may also help to reduce ill-conditioning problems.

**Acknowledgment:** This work was sponsored in part by the Strategic Environmental Research and Development Program and US Army CoE ERDC BT25 and AF25 programs

## References

1. T. H. Bell, B. J. Barrow, and J. T. Miller, "Subsurface discrimination using electromagnetic induction sensors, IEEE Trans. Geosci. Remote Sensing," vol. 39, pp.1286-1293, June 2001
2. Y. Zhang, L. Collins, H. Yu, C. Baun, and Lawrence Carin, "Sensing of Unexploded Ordnance With MagnetometerSensing of Unexploded Ordnance With Magnetometer," IEEE Trans. Geosci. Remote Sensing, Vol. 41, pp.1005-1015, May 2003.
3. F. Shubitidze, K O'Neill, I. Shamatava, K. Sun and K.D. Paulsen, "Analysis of EMI scattering to support UXO discrimination: heterogeneous and multiple objects," Detection and Remediation Technologies for Mines and Minelike Targets VIII (or48), Part of SPIE's 17th Annual International Symposium on AeroSense, , Orlando, Florida, 21-25 April 2003, pp928-939.
4. Shubitidze, K O'Neill, K. Sun, I. Shamatava, Interaction Between Highly Conducting and Permeable Metallic Objects in the EMI Frequency Range, ACES conference Mar 24-28, 2003 Monterey, CA, pp625-631.
5. C. O. Ao, H. Braunsch, K. O'Neill and J. A. Kong "Quasi magnetostatic solution for a conducting and permeable spheroid with arbitrary excitation", IEEE Trans, Geosci. Rem. Sens., Vol. 40, pp. 887-897, April, 2002.
6. B. E. Barrowes, K. O'Neill, T. M. Grzegorzczak, X. Chen and J. A. Kong, "Broadband electromagnetic induction solution for a conducting and permeable spheroid," IEEE Trans. Geosci. Remote Sensing, submitted for publication, 2003.
7. K. Sun, K O'Neill, I. Shamatava, F. Shubitidze, "Application of prolate Spheroid Solutions in Simulation of EMI Scattering with Realistic Sensors and Objects, " ACES conference, Monterey, CA. pp531-537, Mar 24-28, 2003.
8. K. Sun K. O'Neill, L. liu, F. Shubitidze, I. Shamatava, K. D. Paulsen, "Analytical Solutions For EMI Scattering From General Spheroids With Application in Signal Inversion for UXO Discrimination," Detection and Remediation Technologies for Mines and Minelike Targets VIII (or48), Part of SPIE's 17th Annual International Symposium on AeroSense, , Orlando, Florida, 21-25 April 2003, 1035-1045.
9. X. Chen, K. O'Neill, T. M. Grzegorzczak, B. E. Barrowes, C. D. Moss, B. Wu, J. Pacheco, J. A. Kong, "Fundamental mode approach in electromagnetic induction scattering and inversion," Progress in Electromagnetics Research Symposium (PIERS), Honolulu, Hawaii, October 2003
10. F. Shubitidze, K O'Neill, K. Sun, I. Shamatava, and K.D. Paulsen, Fast direct and inverse EMI algorithms for enhanced identification of buried UXO with real EMI data. 2003 IEEE International Geoscience and Remote Sensing Symposium. Toulouse, France, July 21-25, 2003.
11. K. Sun, K. O'Neill, F. Shubitidze, S. A. Haider, and K. D. Paulsen, "Simulation of electromagnetic induction scattering from targets with negligible to moderate penetration by primary fields," IEEE Trans. Geosci. Remote Sensing, Vol. 40, pp.910-927, Apr. 2002.
12. F. Shubitidze, K O'Neill, K. Sun, I. Shamatava, and K.D. Paulsen, A Combined MAS-TSA Algorithm for Broadband Electromagnetic Induction Problems, ACES conference Mar 24-28, 2003 Monterey, CA. pp566-572.
13. I. J. Won, D. A. Keiswetter, D. R. Hanson, E. Novikova and T. M. Hall, "GEM-3: a monostatic broadband electromagnetic induction sensor," Jour. Envir. Eng. Geophysics, Vol. 2, No. 1, pp53-64, 1997
14. D. Marquardt, "An algorithm for least-squares estimation of non-linear parameters," SIAM J. Appl. Math., Vol. 11, pp.431-441, 1963.
15. G. Arfken, "Mathematical methods for Physicists", 3<sup>rd</sup> ed. Orlando, FL: Academic Press, pp. 198-200, 1985
16. Y.V. Kumar, "Image Enhancement techniques in a microwave breast image system", Master thesis, Thayer School of Engineering, Dartmouth College, August, 2001.